

Electrosynthesis of Bi_2O_3 thin films and their use in electrochemical supercapacitors

T.P. Gujar^{a,*}, V.R. Shinde^a, C.D. Lokhande^{a,b}, Sung-Hwan Han^{b,*}

^a Thin Film Physics Laboratory, Department of Physics, Shivaji University, Kolhapur, Maharashtra 416004, India

^b Department of Chemistry, Hanyang University, Sungdong-Ku, Haengdang-dong 17, Seoul, 133-791 Korea

Received 19 February 2006; accepted 15 May 2006

Available online 13 July 2006

Abstract

Bismuth oxide (Bi_2O_3) thin films are grown on copper substrates at room temperature by electrodeposition from an aqueous alkaline nitrate bath. The usefulness of electrochemically deposited Bi_2O_3 for electrochemical supercapacitors is proposed for the first time. The supercapacitor properties of Bi_2O_3 electrode are studied in aqueous NaOH solution. The Bi_2O_3 electrode exhibits very good electrochemical supercapacitive characteristics as well as stability in aqueous NaOH electrolyte. The effect of electrolyte concentration, scan rate, and number of cycles on the specific capacitance of Bi_2O_3 electrodes has been studied. The highest specific capacitance achieved with the electrodeposited Bi_2O_3 films is 98 F g^{-1} .

© 2006 Elsevier B.V. All rights reserved.

Keywords: Bismuth oxide; Electrodeposition; Electrochemical supercapacitor; Specific capacitance

1. Introduction

Bismuth oxide is known to be an important transition metal oxide due to its characteristic parameters such as energy band-gap, refractive index, dielectric permittivity and photoconductivity I_b is suitable for a large range applications, namely, sensors, optical coatings, photovoltaic cells and microwave integrated circuits [1]. An emerging application of Bi_2O_3 may be as an electrode material for electrochemical supercapacitors. Nowadays, considerable interest has been placed on developing electrochemical capacitors with high specific power and energy. The supercapacitors usually consist of electrodes made from highly porous materials (e.g., active carbon) with very high specific surface area or electroactive materials with several oxidation states/structures within the potential window of solvent decomposition [2–4]. Since the pseudocapacitance comes mainly from the reversible redox transitions of the electroactive materials, transition metal oxides are considered as promising materials for supercapacitors [5]. Along with the charge-storage mechanism,

large surface area is an essential property of the electrode material for the attainment of large capacitance. Since nanocrystalline Bi_2O_3 can offer large surface area, electrochemical stability and pseudocapacitive behaviour, it may make a significant contribution to the advancement of supercapacitor technology.

As supercapacitor electrodes, many transition metal oxides, such as RuO_x , NiO_x and IrO_x , have been shown to be excellent materials with their charge-storage mechanisms based on pseudocapacitance [6]. The most success has been achieved using ruthenium oxide. The powder form of amorphous and hydrous ruthenium oxide ($\text{RuO}_2 \cdot x\text{H}_2\text{O}$) electrode have been obtained by the sol–gel method and found to be promising materials for electrochemical capacitors with high specific power and specific energy [7,8]. A maximum specific capacitance of 768 F g^{-1} has been obtained from amorphous ruthenium oxide [9,10]. In thin-film form, Hu and Huang [4] and Park et al [11] (specific capacitance = 788 F g^{-1}) have successfully employed electrochemically deposited hydrous ruthenium oxide for electrochemical supercapacitors. Though the ruthenium oxide ($\alpha\text{-RuO}_2 \cdot x\text{H}_2\text{O}$) exhibits excellent pseudocapacitive behaviour with large specific capacitance and good reversibility, the low abundance and high cost of the precious metal are major limitations to commercial application [12]. Therefore, there is a strong need to develop a low-cost material with a significant value of capacitance. Con-

* Corresponding authors. Tel.: +91 231 2690571; fax: +91 231 2691533.

E-mail addresses: gujar_tp@yahoo.com (T.P. Gujar),

l.chandrakant@yahoo.com (C.D. Lokhande),

shhan@hanyang.ac.kr (S.-H. Han).

sequently, there are increasing attempts to develop cost-effective supercapacitors based on non-noble transition metal oxides, e.g., oxides of manganese [13], nickel [14] and cobalt [15,16].

In the present work, Bi_2O_3 thin films are grown at room temperature by electrodeposition from an aqueous medium of bismuth nitrate and for the first time, exploited as a supercapacitor electrode in aqueous NaOH electrolyte. The Bi_2O_3 films are characterized in terms of their structural and electrochemical supercapacitive characteristics.

2. Experimental

The bismuth oxide films were electrodeposited at room temperature from an aqueous solution of 0.2 M bismuth (III) nitrate complexed with 0.2 M tartaric acid solution. The pH of the solution was adjusted to ~ 12 by addition of aqueous NaOH solution. The solution was prepared in freshly prepared double-distilled water. Mirror polished and ultrasonically cleaned copper was used as a substrate. Cyclic voltammetry (CV) studies were performed to study the oxidation and reduction mechanisms in the electrolytic bath within the potential range of 0 to -1 V. (Note, all voltages are reported with respect to a saturated calomel reference electrode, SCE.) All the voltammetric curves were obtained with a scanning potentiostat (Model-273 A EG and G) by forming a conventional three-electrode cell. The working electrode was a well-cleaned substrate of dimensions $1 \text{ cm} \times 4 \text{ cm} \times 0.1 \text{ cm}$. The counter electrode was polished graphite plate of dimensions $1.5 \text{ cm} \times 4 \text{ cm} \times 1 \text{ cm}$. The reference electrode was a saturated calomel electrode (SCE). The preparative parameters were optimized to obtain feasible films for supercapacitor applications.

With optimized parameters, deposition of bismuth oxide was carried out in galvanostatic mode using chronopotentiometry. A blackish bismuth oxide film was obtained on the copper substrate. The film thickness was determined by the weight difference method using a sensitive microbalance. Structural analysis was carried out with a Philips diffractometer (Philips PW-3710) using a copper target of wavelength 1.5405 \AA . Supercapacitive studies of the bismuth oxide on copper substrates were performed with cyclic voltammetry using a 273A EG & G Princeton Applied Research potentiostat. The electrochemical cell used a platinum counter electrode, a saturated calomel electrode reference electrode in NaOH electrolyte. The effect of electrolyte concentration and scan rate on the capacitance was examined. For charge–discharge studies of the bismuth oxide electrode, a cell was assembled with same configuration and 1 M NaOH electrolyte and operated under the constant current of 1 mA cm^{-2} in the voltage range of 0 and $+0.7 \text{ V}$.

3. Results and discussions

3.1. Cyclic voltammetry curve and film formation

Cyclic voltammetry is a versatile electroanalytical technique for the study of electroactive species. The procedure consists of linearly cycling the potential of an electrode immersed in an unstirred solution while measuring the resulting current. Thus, a

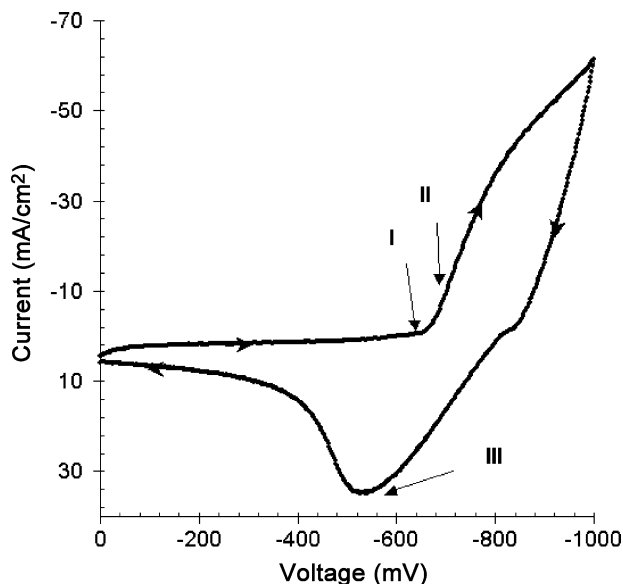
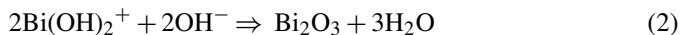


Fig. 1. Cyclic voltammogram of bismuth oxide from aqueous nitrate bath on a copper substrate.

voltammogram is a display of current versus potential in which the direction of the potential is reversed at the end of the first scan. It is a powerful tool for the determination of formal redox potentials, the detection of chemical reactions that precede or follow the electrochemical reaction, and the evaluation of electron transfer kinetics.

Cyclic voltammogram were obtained from an electrolyte bath containing 0.2 M $\text{Bi}(\text{NO}_3)_3$ complexed with tartaric acid and at a pH ~ 12 adjusted using aqueous NaOH and deposited on a Cu substrate at room temperature. A typical CV in the range of 0 to -1 V SCE^{-1} at a scan rate 20 mV s^{-1} is shown in Fig. 1. Reduction and oxidation peaks are seen in the forward and reverse scans, respectively. The hydroxide ions in the solution, produced due to the high alkalinity of the solution, are attracted towards the cathode at high potentials and Bi_2O_3 is produced from $\text{Bi}(\text{OH})_2^+$. Thus, the reduction peak at 0.7 V corresponds to reduction of Bi_2O_3 to $\text{Bi}(\text{OH})_2^+$. At this peak, the higher potential and alkaline medium assists the formation of Bi_2O_3 , which takes place according to:



Thus, by analyzing CV plot, the estimated deposition current for the formation of Bi_2O_3 films on to the Cu substrate is 12 mA cm^{-2} .

3.2. Thickness measurements

The thickness of the Bi_2O_3 film was measured by the gravimetric weight difference method. The density of the deposited material is assumed to be the same as that of the bulk material ($\rho = 9.17 \text{ g cm}^{-3}$ for Bi_2O_3 films). The variation of thickness with deposition time is shown in Fig. 2. As the deposition time is increased, the film thickness also increases. A maximum thick-

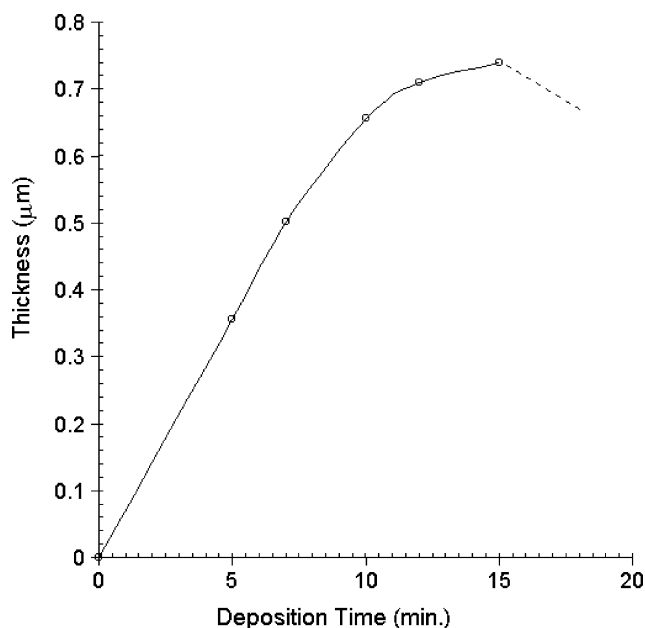


Fig. 2. Variation of film thickness with deposition time. Dotted line indicates peeling of film from substrate.

ness of $0.74 \mu\text{m}$ is attained after a deposition of 15 min. Above 15 min, the film peeled off from the substrate and no further deposition is observed. This can be attributed to the tensile stress that tends to cause delamination when film becomes thick [17,18].

3.3. X-ray diffraction studies (XRD)

The bismuth oxide film on the copper substrate was characterized by X-ray diffraction in the 2θ range $20\text{--}80^\circ$. The XRD pattern is shown in Fig. 3 and Table 1 gives a comparison of the observed 'd' values of Bi_2O_3 with 'd' values taken from stan-

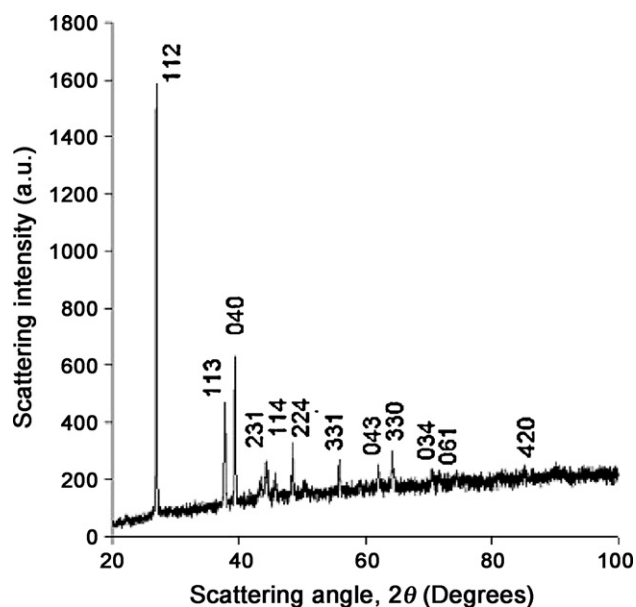


Fig. 3. X-ray diffraction pattern of thin film of Bi_2O_3 on copper substrate.

Table 1

Comparison of observed 'd' values with standard 'd' values for a thin film of Bi_2O_3 on a copper substrate

Serial no.	Observed 'd' (Å)	Standard 'd' (Å)	(hkl)
1	3.30	3.29	112
2	2.38	2.38	113
3	2.03	2.03	040
4	1.98	1.98	231
5	1.87	1.87	311
6	1.81	1.81	114
7	1.64	1.64	224
8	1.56	1.56	331
9	1.51	1.52	043
10	1.49	1.49	330
11	1.44	1.45	034
12	1.33	1.33	061
13	1.31	1.31	161
14	1.27	1.27	420

dard data cards [ASTM data Card No. 76-1730]. There is good agreement between the observed and standard 'd' values. This confirms the formation of polycrystalline monoclinic Bi_2O_3 . It should be noted that the relative peak intensity of the diffraction arising from the (112) plane is much stronger than other peaks that correspond to other planes. This reveals that Bi_2O_3 is oriented along the (112) plane. Bohannan et al. [19] have reported the textured growth of bismuth oxide on a gold substrate by an electrodeposition method. They observed strong (111) and (220) preferred orientations on single crystalline gold substrates. By contrast, Switzer et al. [20] obtained randomly oriented nanoscale crystallites of $\delta\text{-Bi}_2\text{O}_3$ from electrodeposition on stainless steel and glassy carbon substrates. The crystallite size of the (112) plane oriented Bi_2O_3 film particles was estimated using Scherrer's formula:

$$D = 0.9\lambda / \beta \cos \theta \quad (3)$$

where λ is X-ray wavelength, θ the Bragg angle and β is the full width of the diffraction line at half of the maximum intensity. The crystallite size of Bi_2O_3 is estimated to be about 39 nm. The crystalline nature of the electrode, however limits supercapacitor performance only through the surface charge transfer reaction.

3.4. Supercapacitive studies

The electrodeposited bismuth oxide films were used in electrochemical supercapacitors. Supercapacitive performance was tested by means of cyclic voltammetry and chronopotentiometry (CP).

3.4.1. Cyclic voltammogram of bismuth oxide electrode

Cyclic voltammograms of a bismuth oxide electrode of thickness $0.21 \mu\text{m}$ in aqueous electrolytes, viz., 1.0 M solutions of NaOH, KOH, Na_2SO_3 , Na_2SO_4 , NaCl and KCl, were studied in the voltage range of 0 to -800 mV . In all cases, the electrode exhibited symmetrical CV characteristics in the forward and reverse sweeps. The NaOH electrolyte was found to give the largest current value, namely, two to four times greater than that of the other electrolytes. A typical CV for the electrode-

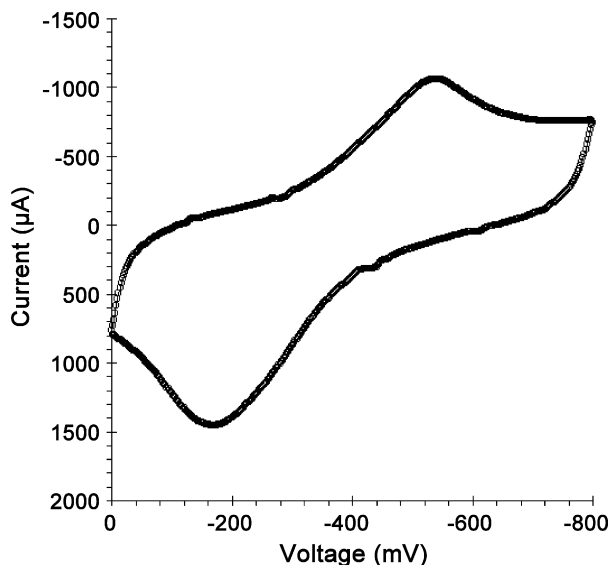


Fig. 4. Typical cyclic voltammogram of Bi_2O_3 electrode deposited on copper substrate in 1 M NaOH electrolyte at scan rate of 100 mV s^{-1} .

posited Bi_2O_3 electrode in 1 M NaOH electrolyte at a scan rate of 100 mV s^{-1} is shown in Fig. 4. The results indicate a good capacitive response from the electrode. Note that, one pair of redox peaks on this cyclic voltammogram is seen, which indicates redox transitions of bismuth oxide between different valence states. News since the voltammetric responses on the positive sweeps are symmetrical with their counterparts on the negative sweeps, this oxide can be employed as an electrode material for electrochemical supercapacitors. When a potential difference is applied across the electrode in a solution, redox reactions occur and the charge builds up on the surface of electrode. Due to electrostatic interactions, ions in the solution migrate to the electrode to counterbalance the charge on the electrode, i.e., protons travel from one electrode to the other through the electrolyte during charge and discharge. The movement of electrons occurs at the same time through the current source or the external load. Thus, the current–voltage profile of the Bi_2O_3 electrode is symmetrical.

The interfacial capacitance and specific capacitance were calculated from:

$$C = \frac{I}{(dv/dt)} \quad (4)$$

where I is the average current in amperes; dv/dt is the scanning rate in mV s^{-1} .

The specific capacitance (F g^{-1}) of the electrode is obtained by dividing the capacitance by the weight when dipped in electrolyte and the interfacial capacitance is calculated by dividing the capacitance by the area of the electrode dipped in the electrolyte. The obtained values are 0.013 F cm^{-2} and 68 F g^{-1} , respectively. This performance is definitely better than newly employed materials for supercapacitors. For example, for SnS nanorods, Jayalakshmi et al. [21] obtained a maximum capacitance of less than 20 F g^{-1} in NaCl and KOH electrolytes. Wu [22] also found a maximum capacitance of less than 20 F g^{-1}

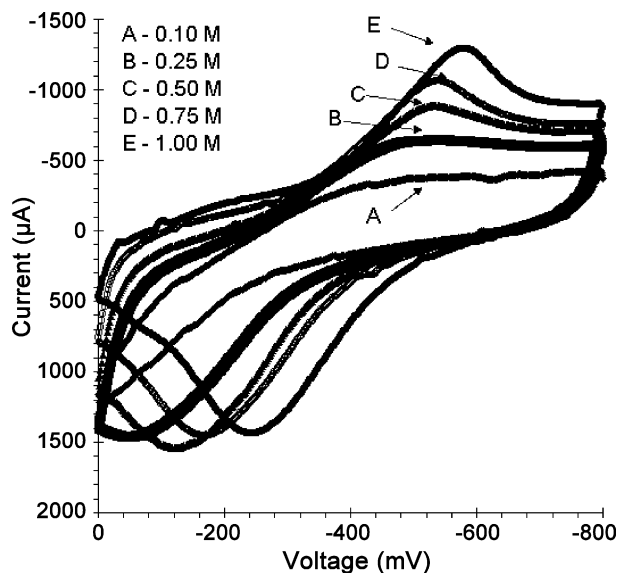


Fig. 5. Cyclic voltammograms of Bi_2O_3 electrode in different concentrations of NaOH electrolyte. Scanning rate 100 mV s^{-1} .

for SnO_2 xerogels [22]. The specific capacitance of the Bi_2O_3 electrode is smaller than that of conventional electrochemically deposited electrodes such as RuO_2 ($>500 \text{ F g}^{-1}$) [4,11,23,24] and MnO_2 ($>200 \text{ F g}^{-1}$) [7,25]. The main reason that limits the capacitance of Bi_2O_3 may be the crystalline structure of the electrode. This is because the lattice of the crystalline material is rigid and is difficult to expand when the ions are inserted during the redox reaction. The best example of this fact is of RuO_2 , i.e., the capacitance of amorphous RuO_2 is reported to be about 700 F g^{-1} , while that of crystalline RuO_2 is about 380 F g^{-1} [9].

3.4.2. Effect of electrolyte concentration

The effect of electrolyte concentration was studied by keeping the scan rate and potential scanning range constant but changing the NaOH concentration from 0.1 to 1 M. The CV curves of Bi_2O_3 electrode at a scan rate 100 mV s^{-1} within the potential range of 0 to -800 mV in NaOH electrolyte of different concentrations are presented in Fig. 5. The current under the curve increases as the NaOH concentration is increased from 0.1 to 1 M. Thereafter the current under the curve is fairly constant. It is seen that the voltammograms are more distorted than those in Fig. 4 with decrease in electrolyte concentration. At low concentrations of NaOH, i.e., for 0.1–0.25 M, the CV curves have no well-resolved redox peaks. As the electrolyte concentration is increased from 0.5 to 1.0 M, redox peaks emerged, and with concentration the difference in redox peak potential decreases. This is due to free-electrolyte starvation since, for the amount of electrolyte present in the solutions almost all the ions become adsorbed at the high-area interface and there by enhance the internal resistance effect towards full state-of-charge through a combination of the usual distributed resistance effects. Similar type of behaviour has been observed by Zheng and Jow [26], and by Convey and Pell [27]. For concentrations above 1.0 M, no change in the CV curves is observed. The variation of specific and interfacial capacitance with concentration of

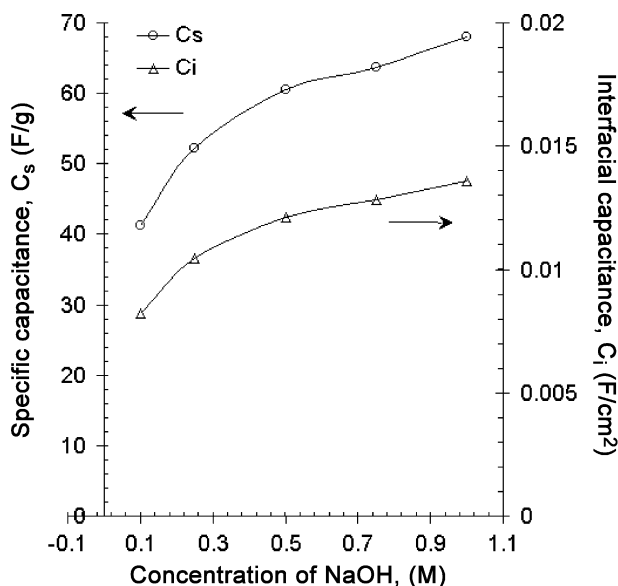


Fig. 6. Variation of specific and interfacial capacitance of Bi_2O_3 electrode at different concentrations of NaOH electrolyte. Scanning rate was 100 mV s^{-1} .

electrolyte is shown in Fig. 6. The specific and interfacial capacitances increase with increasing concentration of electrolyte. The maximum values of interfacial and specific capacitances are 0.013 F cm^{-2} and 68 F g^{-1} , respectively.

3.4.3. Effect of scan rate

The effect of scan rate on an electrochemical supercapacitor formed by electrodeposited bismuth oxide was studied in 1.0 M NaOH in the voltage range of 0 to -800 mV . The resulting cyclic voltammograms at different scan rates are presented in Fig. 7. The current under the curve slowly increases with scan rate. This shows that the voltammetric currents are directly proportional to the scan rate and thereby indicates ideal capacitive behaviour

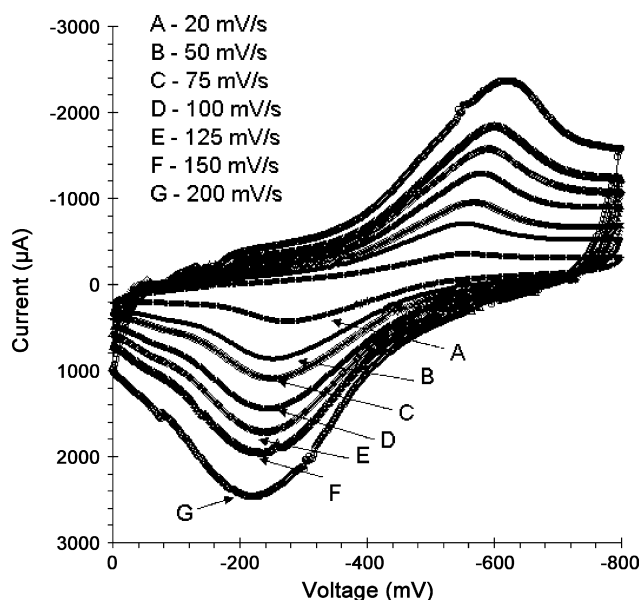


Fig. 7. Cyclic voltammograms of Bi_2O_3 electrode at different scanning rates. Concentration of NaOH electrolyte 1.0 M .

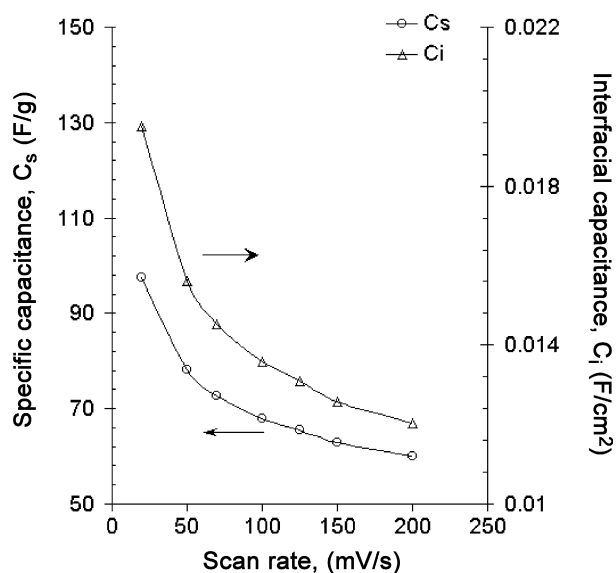


Fig. 8. Variation of specific and interfacial capacitance of Bi_2O_3 electrode at different scan rates. Concentration of NaOH electrolyte 1.0 M .

[5]. The variation of specific and interfacial capacitances with the scan rate is given in Fig. 8. It is seen that the specific and interfacial capacitances decrease from 98 F g^{-1} and 0.022 F cm^{-2} to 60 F g^{-1} and 0.012 F cm^{-2} , respectively, as the scan rate is increased from 20 to 200 mV s^{-1} . The decrease in capacitance has been attributed to the presence of inner active sites that cannot sustain the redox transitions completely at higher scan rates. This is probably due to the diffusion effect of protons within the electrode [28]. The decreasing trend of the capacitance suggests that parts of the surface of the electrode are inaccessible at high charging–discharging rates. Hence, the specific capacitance obtained at the slowest scan rates is believed to be closest to that of full utilization of the electrode material.

3.4.4. Stability of bismuth oxide electrode

The CV curves of a bismuth oxide electrode for different number of cycles are presented in Fig. 9. The data show that a very stable material has been synthesized by using electrodeposition. The system can withstand over 1000 cycles without any significant decrease in capacity. This demonstrates that the material is suitable for energy-storage applications. The specific capacitance and interfacial capacitance decrease only by small values with cycling (see Fig. 10). As revealed from this data, the specific capacitance of all the electrodes declines very fast during the first 25 cycles but remains almost constant thereafter (until 1000 cycles). The active material may be lost, caused by dissolution and/or detachment, during the early charge–discharge cycles [29].

3.4.5. Charge–discharge mechanism

The charge–discharge behaviour of bismuth oxide electrodes was studied by chronopotentiometry at a constant current of 1 mA cm^{-2} between 0 and $+0.7 \text{ V}$. Non-symmetrical behaviour of voltage–time curve is seen, i.e., an IR drop is observed (Fig. 11). The discharge profile usually contains two parts, newly, a sudden voltage drop (linear portion parallel to y-axis)

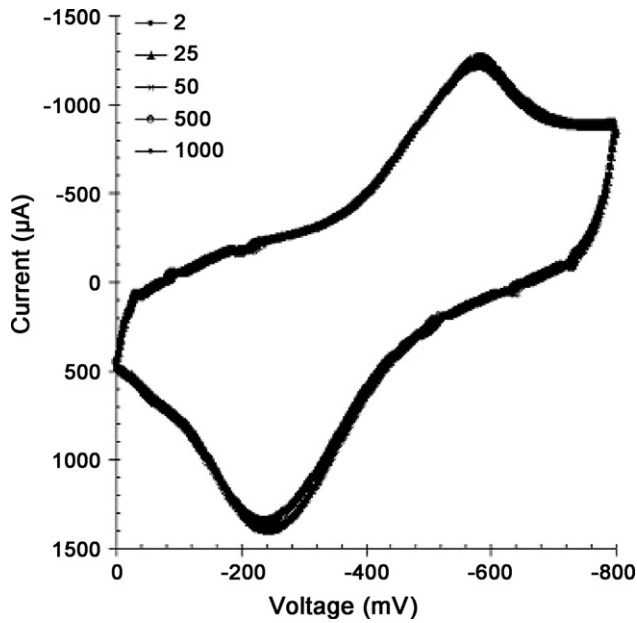


Fig. 9. Cyclic voltammograms of Bi_2O_3 electrode at different cycles. Scanning rate and concentration of NaOH electrolyte 100 mV s^{-1} and 1.0 M , respectively.

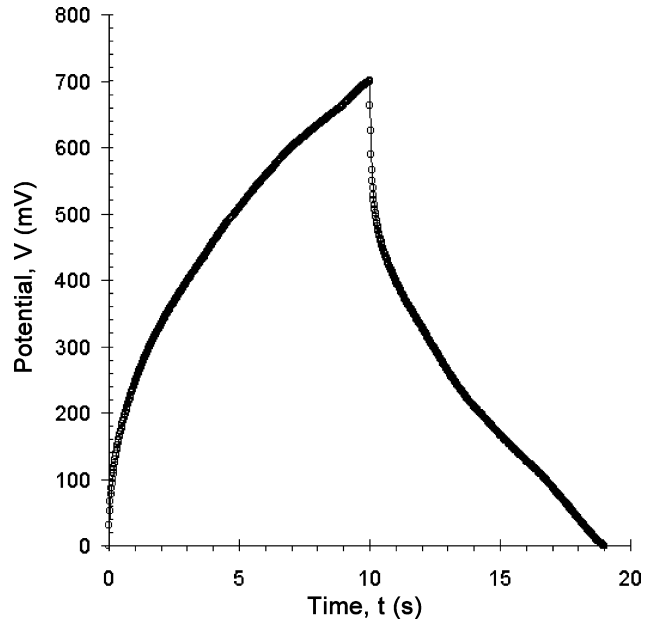


Fig. 11. Charge-discharge curves of Bi_2O_3 supercapacitor in 1.0 M NaOH electrolyte.

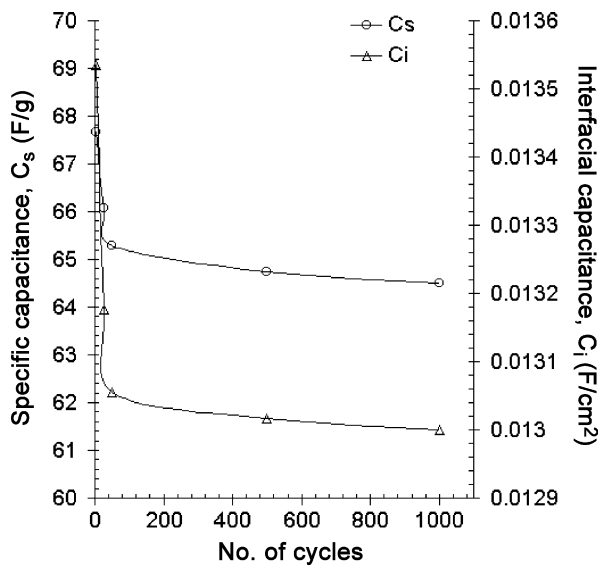


Fig. 10. Variation of specific and interfacial capacitance of Bi_2O_3 electrode at different cycles. Scanning rate and concentration of NaOH electrolyte 100 mV s^{-1} and 1.0 M , respectively.

representing the voltage change due to the internal resistance and a capacitive component (curved portion) related to the voltage change due to change in energy within the capacitor [21].

The average capacitance of the Bi_2O_3 electrode was calculated according to the following relation:

$$C = I \times \left(\frac{\Delta t}{\Delta V} \right) \quad (5)$$

where Δt is the time duration (s) of the discharge process; ΔV (V) is the voltage range. From charge-discharge profile, the specific capacitance is estimated to be 57 F g^{-1} , which is comparable with the values obtained from CV curves.

4. Conclusions

Bismuth oxide films have been deposited on a copper substrate at room temperature using an electrochemical method. Electrochemically-deposited thin films of bismuth oxide have been successfully employed as supercapacitor electrodes and give satisfactory performance, high electrochemical reversibility, good stability, high power, and high specific capacitance. Though the Bi_2O_3 films are crystalline with a monoclinic crystal structure, they are capable of giving a specific capacitance of 98 F g^{-1} . Although the performance of the Bi_2O_3 electrode is poor compared with a conventional expensive RuO_2 electrode, it is possible that further research to overcome its limitations will bring it to such a position as to make it a promising candidate for use in supercapacitors.

Acknowledgements

Authors are grateful to CSIR, New Delhi, for providing financial support through the scheme no. 03(1021)/05/EMR-II. VRS thanks Shivaji University, Kolhapur, for the award of Departmental Research Fellowship (DRF).

References

- [1] T.P. Gujar, V.R. Shinde, C.D. Lokhande, R.S. Mane, S.-H. Han, Appl. Surf. Sci. 250 (2005) 161.
- [2] B.E. Conway, Electrochemical Supercapacitors, Kluwer/Plenum Publishing Co., New York, 1999.
- [3] J.P. Zheng, J. Huang, T.R. Jow, J. Electrochem. Soc. 144 (1997) 2026.
- [4] C.C. Hu, Y.H. Huang, J. Electrochem. Soc. 146 (1999) 2465.
- [5] C.C. Hu, T.W. Tsou, Electrochem. Commun. 4 (2002) 105.
- [6] H.K. Kim, T.Y. Seong, J.H. Lim, W.L. Cho, Y.S. Yoon, J. Power Sources 102 (2001) 167.
- [7] J.P. Zheng, T.R. Jow, J. Power Sources 62 (1996) 155.

- [8] J.P. Zheng, *Electrochem. Solid State Lett.* 2 (1999) 359.
- [9] I.D. Raistick, in: J. McHardy, F. Ludwig (Eds.), *The Electrochemistry of Semiconductors and Electronics-Processes and Devices*, Noyes, NJ, USA, 1992, p. 297.
- [10] J.P. Zheng, T.R. Jow, *J. Electrochem. Soc.* 142 (1995) L6.
- [11] B.O. Park, C.D. Lokhande, H.S. Park, K.D. Jung, O.S. Joo, *J. Power Sources* 134 (2004) 148.
- [12] M. Wu, G.A. Snook, G.Z. Chen, D.J. Fray, *Electrochem. Commun.* 6 (2004) 499.
- [13] H.Y. Lee, S.W. Kim, H.Y. Lee, *Electrochem. Solid State Lett.* 4 (2001) A19.
- [14] K.C. Liu, M.A. Anderson, *J. Electrochem. Soc.* 143 (1996) 124.
- [15] C. Lin, J.A. Ritter, B.N. Popov, *J. Electrochem. Soc.* 145 (1998) 4097.
- [16] V.R. Shinde, S.B. Mahadik, T.P. Gujar, C.D. Lokhande, *Appl. Surf. Sci.* (2006) (available online).
- [17] J.A. Thornton, *J. Vac. Sci. Technol.* A4 (1986) 3059.
- [18] Y. Kitamoto, M. Abe, *J. Phys. IV France* 7 (1997) C1–C595.
- [19] E.W. Bohannon, C.C. Jaynes, M.G. Shumsky, J.K. Barton, J.A. Switzer, *Solid State Ionics* 131 (2000) 97.
- [20] J.A. Switzer, M.G. Shumsky, E.W. Bohannon, *Science* 284 (1999) 293.
- [21] M. Jayalakshmi, M.M. Rao, B.M. Choudary, *Electrochem. Commun.* 6 (2004) 1119.
- [22] N.L. Wu, *Mater. Chem. Phys.* 75 (2002) 6.
- [23] C.C. Hu, K.H. Chang, *Electrochim. Acta* 45 (2000) 2685.
- [24] C.C. Hu, Y.H. Huang, *Electrochim. Acta* 46 (2001) 3431.
- [25] C.C. Hu, T.W. Tsou, *Electrochim. Acta* 47 (2002) 3523.
- [26] J.P. Zheng, T.R. Jow, *J. Electrochem. Soc.* 144 (1997) 2417.
- [27] B.E. Conway, W.G. Pell, *J. Power Sources* 105 (2002) 169.
- [28] K.H. Chang, C.C. Hu, *J. Electrochem. Soc.* 151 (2004) A958.
- [29] R. Kotz, M. Carlen, *Electrochim. Acta* 45 (2000) 2483.